

# Reprocessing Post-Consumer Polyurethane Foam Using Carbamate

## Exchange Catalysis and Twin-Screw Extrusion

Daylan T. Sheppard,<sup>1</sup> Kailong Jin<sup>2</sup>, Leslie Hamachi<sup>1</sup>, William Dean<sup>2</sup>, David J. Fortman<sup>1,3</sup>,  
Christopher J. Ellison<sup>2</sup>, and William R. Dichtel<sup>1,\*</sup>

<sup>1</sup>*Department of Chemistry, Northwestern University,  
2145 Sheridan Rd., Evanston, Illinois 60208, USA*

<sup>2</sup>*Department of Chemical Engineering and Materials Science,  
University of Minnesota, Minneapolis, MN 55455, USA*

<sup>3</sup>*Department of Chemistry and Chemical Biology, Cornell University,  
Baker Laboratory, Ithaca, New York, 14853 USA*

## Supplementary Information

### Table of Contents

<b>A.</b> Materials & General Methods	S2
<b>B.</b> Synthetic Procedures	S4
<b>C.</b> Characterization Tables and Figures	S5
<b>D.</b> References	S23

## A. Materials and General Methods

**Materials.** All reagents were purchased from Sigma-Aldrich or Fisher Scientific. Polyols were dried at 90 °C under 20 mTorr vacuum for at least 24 hours prior to use for film synthesis. All other reagents were used without further purification unless otherwise specified. Dichloromethane ( $\text{CH}_2\text{Cl}_2$ ) and toluene were purchased from Fisher Scientific and purified using a custom-built alumina-column based solvent purification system.

**Instrumentation.** Infrared spectra were recorded on a Thermo Nicolet iS10 equipped with a ZnSe ATR attachment. Spectra were uncorrected.

Solid-state NMR spectra were recorded on a 400 MHz Bruker Avance III using a standard Bruker 4 mm HX probe at ambient temperature.

Thermogravimetric analysis (TGA) was performed on a Mettler Toledo SDTA851 Thermogravimetric Analysis System using 5-10 mg of sample. Samples were heated under a nitrogen atmosphere at a rate of 10 °C/min from 25 °C to 600 °C.

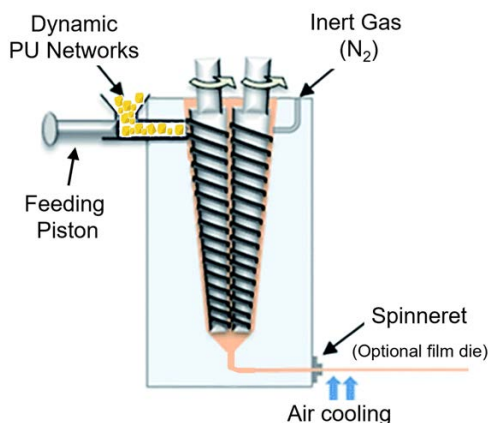
Differential scanning calorimetry (DSC) was performed on a TA Instruments DSC250 Differential Scanning Calorimeter. Samples (5-10 mg) were heated at a rate of 10 °C/min to at least 150 °C to erase thermal history, cooled to -80 °C at 10 °C/min, and then heated to at least 120 °C. All data shown are taken from the second heating ramp. The glass transition temperature ( $T_g$ ) was calculated from the maximum value of the derivative of heat flow with respect to temperature.

Dynamic mechanical thermal analysis (DMTA) was performed on a TA Instruments RSA-G2 analyzer (New Castle, DE) using rectangular (*ca.* 0.75 mm (T)  $\times$  5 mm (W)  $\times$  20 mm (L) and a gauge length of 10 mm). The axial force was adjusted to 0 N and a strain adjust of 30% was set with a minimum strain of 0.05%, a maximum strain of 5%, and a maximum force of 1 N in order to prevent the sample from buckling or going out of the specified strain. Furthermore, a force tracking mode was set such that the axial force was twice the magnitude of the oscillation force. A temperature ramp was then performed from 30 °C to 160 °C at a rate of 5 °C/min, with an oscillating strain of 0.05% and an angular frequency of 6.28 rad s<sup>-1</sup> (1 Hz). The  $T_g$  was calculated from the maximum value of the loss modulus ( $E''$ ).

Stress relaxation analysis (SRA) was performed on a TA Instruments RSA-III analyzer (New Castle, DE) using rectangular films (*ca.* 1.0 mm (T)  $\times$  4 mm (W)  $\times$  5 mm (L) and a Gauge length of 9 mm). The SRA experiments were performed with strain control at specified

temperature (140 to 160 °C). The samples were allowed to equilibrate at this temperature for approximately 10 minutes, after which the axial force was then adjusted to 0 N. Each sample was then subjected to an instantaneous 5% strain. The stress decay was monitored, while maintaining a constant strain (5%), until the stress relaxation modulus had relaxed to at least 37% ( $1/e$ ) of its initial value. This was performed three consecutive times for each sample. The activation energy ( $E_a$ ) was determined using the methodology in literature.<sup>1</sup>

To reprocess the materials, the polymer was ground into small pieces using a Cuisinart Grind Central<sup>®</sup> coffee grinder. The ground polymer was spread between two aluminum plates in a 1.0 mm thick aluminum mold. This assembly was placed in PHI 30-ton manual press preheated to the desired temperature and allowed to thermally equilibrate for 1 minute. The material was compressed at 8 MPa of pressure for 30 s, then the pressure was released, and this was repeated 2x to enable removal of air bubbles. The material was then compressed at 8 MPa for 12 minutes. The homogenous polymer was removed from the mold, and specimens for DMTA were cut into rectangular films or tensile bars.



Reprocessing via microcompounding: Ground polyurethane powders were fed into a recirculating, conical twin-screw batch mixer (DSM Xplore, 5 mL capacity) operated at 100 rpm with a steady nitrogen purge. The operating temperatures for model and commercial PU foams were 200 and 220 °C, respectively. The residence time was estimated to be ~1 min. The material was then extruded through a 2.5 mm diameter die (into a cylinders) or a 1 mm thick film die (into continuous films) and air cooled.

Scanning Electron Microscopy: Polyurethane foams and films were secured to a flat or 90° aluminum sample holder, coated with 5 nm of osmium, and imaged with a Hitachi S4800-II cFEG SEM.

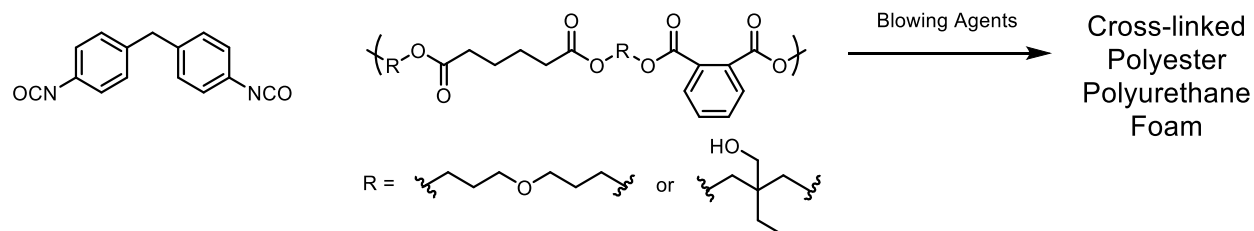
Optical microscopy was performed on an Olympus SZX16 microscope.

### Safety Statement:

No unexpected and unusually high safety hazards were encountered

## B. Synthetic Procedures

### Scheme S1: Synthesis of Cross-linked Polyester Polyurethane Foam



**Synthesis of Crosslinked Polyester Polyurethane Foam:** To a plastic cup was added poly[trimethylolpropane/di(propylene glycol)-*alt*-adipic acid/phthalic anhydride] polyol (200 eq. wt., 10 g, 50 mmol -OH), blowing agents isopentane (300 mg) or H<sub>2</sub>O (300 mg, 16.7 mmol), and dibutyltin dilaurate (111 mg, 0.35 mol % with respect to -NCO). Ground solid 4,4'-methylenebis(phenyl isocyanate) (MDI) (6.26 g, 25.0 mmol) was added and mixed vigorously. The mixture was allowed to sit for one hour to gel and rise. The resulting bulk polymer was transferred to an aluminum pan (104 mm D x 15 mm H) and placed in a vacuum oven at 90 °C at 20 mTorr to immediately expand and cure for 48 hours. The foam was post cured at 150 °C for 1 hour to ensure full cross-linking.

### Control PU Film:

FT-IR (solid, ATR) 3307 (N-H stretch), 2917, 1708 (C=O stretch), 1597, 1529 (N-H deformation), 1457, 1412, 1377, 1308, 1219, 1066, 1017, 816, 766 cm<sup>-1</sup>.

### Physically Blown PU Foam:

FT-IR (solid, ATR) 2932, 1723 (C=O stretch), 1596, 1530 (N-H deformation), 1511, 1456, 1412, 1377, 1307, 1219, 1124, 1063, 1017, 816, 767, 745, 705 cm<sup>-1</sup>.

### Chemically Blown PU Foam:

FT-IR (solid, ATR) 3334 (N-H stretch), 2918, 1724 (C=O stretch), 1596, 1531 (N-H deformation), 1511, 1459, 1412, 1377, 1309, 1220, 1065, 1017, 816, 766 cm<sup>-1</sup>.

### Post-synthetic introduction of catalyst to model PU film or foam:

One gram of model foam or film was suspended in 10 mL of benchtop dichloromethane. To the suspension DBTDL (300 mg) was added and the resulting 30 mg/mL catalyst solution was stirred overnight. The resulting swollen polymer was filtered, collected, and placed in a vacuum oven at 90 °C at 20 mTorr for 24 hours to remove residual dichloromethane. When scaling up to multigram

amounts, the amount of 30 mg/mL solvent was adjusted to match the polymer to solvent ratio of 100 mg/mL.

### **Post-synthetic introduction of catalyst to commercial PU film or foam:**

Thirty grams of commercial foam was suspended in 1.5L of benchtop dichloromethane. To the suspension DBTDL (4.5 grams) was added and the resulting 30 mg/mL catalyst solution was stirred overnight. The resulting swollen polymer was filtered, collected, and placed in a vacuum oven at 90 °C at 20 mTorr for 24 hours to remove residual dichloromethane.

### **C. Characterization Tables and Figures**

Area under  $\tan(\delta)$  calculation using the rectangle method:

$$\int_{T_i}^{T_f} \tan(\delta) dT$$

Where  $T_f$  is the final temperature and  $T_i$  is the initial starting temperature

$$\sum_{n=1}^{T_f} \left( \frac{\tan(\delta)_n + \tan(\delta)_{n+1}}{2} \right) * (T_{n+1} - T_n)$$

All areas were calculated over the entire temperature range of the measurement using the rectangular method.

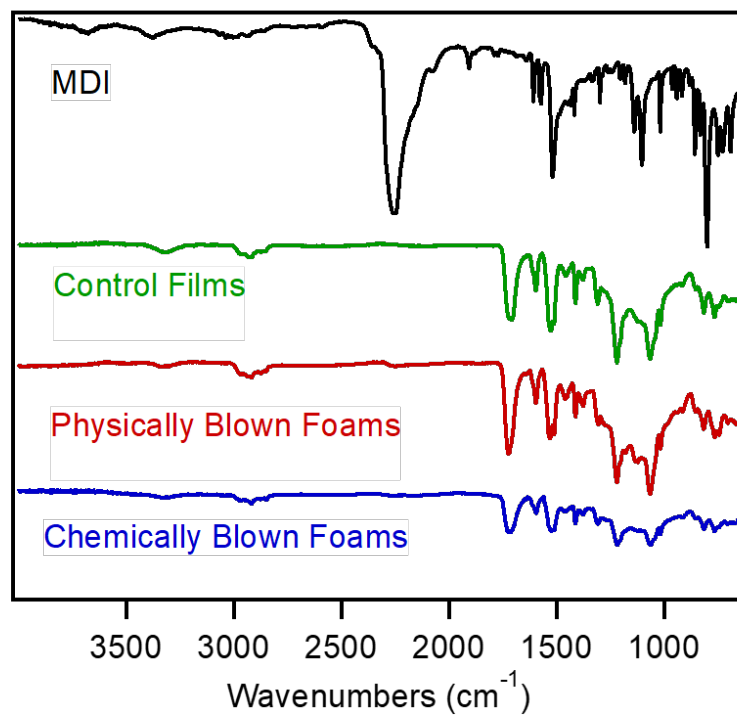


**Figure S1.** FT-IR spectra of 4,4'-methylenebis(phenylisocyanate) (black), as-synthesized PU films (green), physically blown PU foam (red) and chemically blown PU foam (blue).

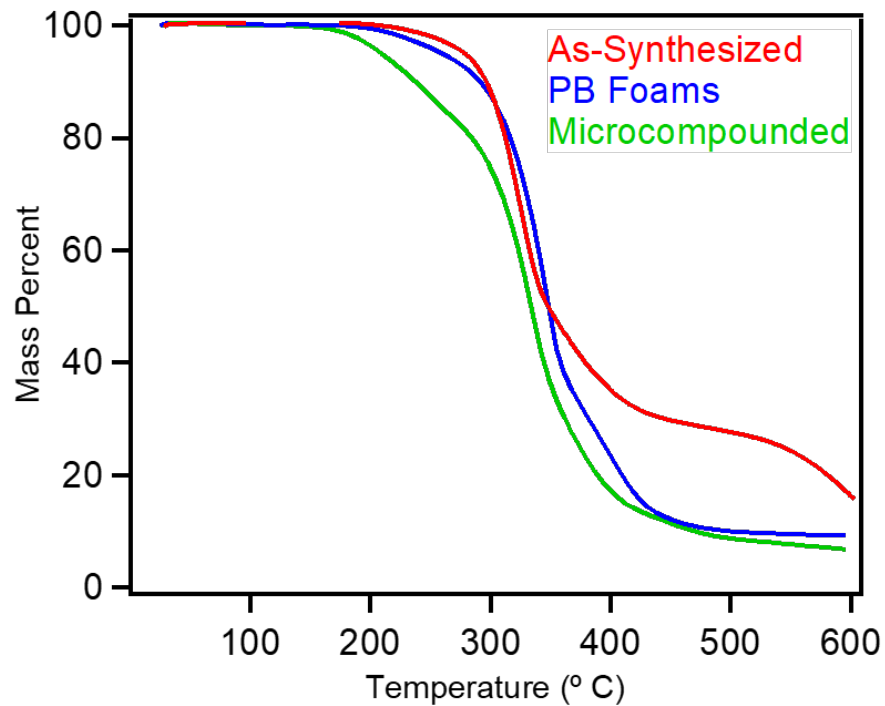


**Figure S2.** Thermogravimetric analysis of as-synthesized films (red), physically blown PU foams (blue), and microcompounded physically blown PU foams (green).

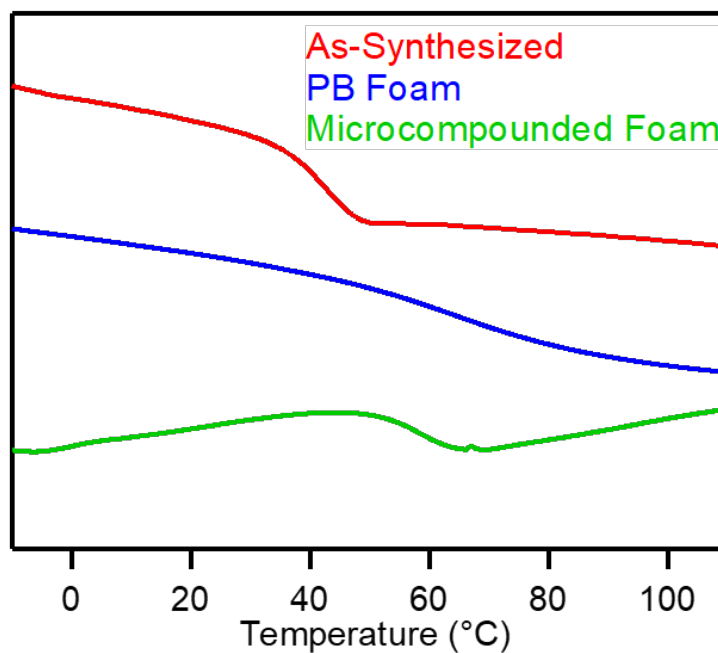


**Figure S3.** Differential scanning calorimetry of as-synthesized films (red), physically blown PU foams (blue), and microcompounded physically blown PU foams (green).

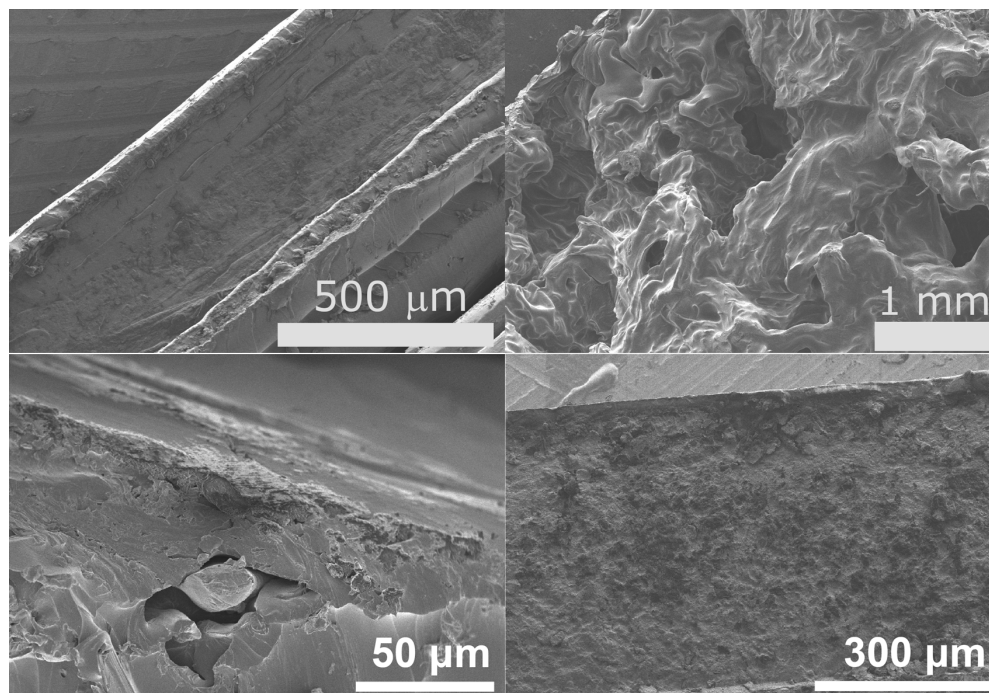


**Figure S4.** SEM images of synthesized model PU film (top left), model PB foam (top right), model PB foam compression molded (bottom left), and model PB foam microcompounded (bottom right).

**Table S1.** The weight percent of Sn measured in various PU materials using ICP-OES.

PU materials	Before Post-synthetic treatment	After Post-synthetic treatment	After microcompounding
As-Synthesized PU Films	<0.01%	0.56%	-
As-Synthesized PB Foam	0.14%	0.92%	0.79%
Commercial Foam	0.02%	0.64%	0.47%

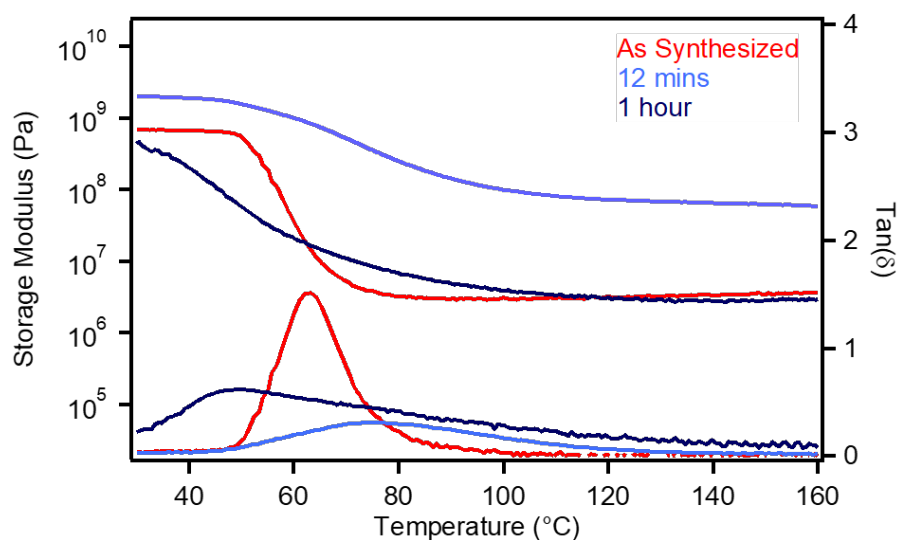


**Figure S5.** DMTA of compression molded PU film (red), compression molded PB foams for 12 mins (light blue), and compression molded PB foams at 1 hour (dark blue). Compression molded materials were swollen in catalyst solution prior to processing.



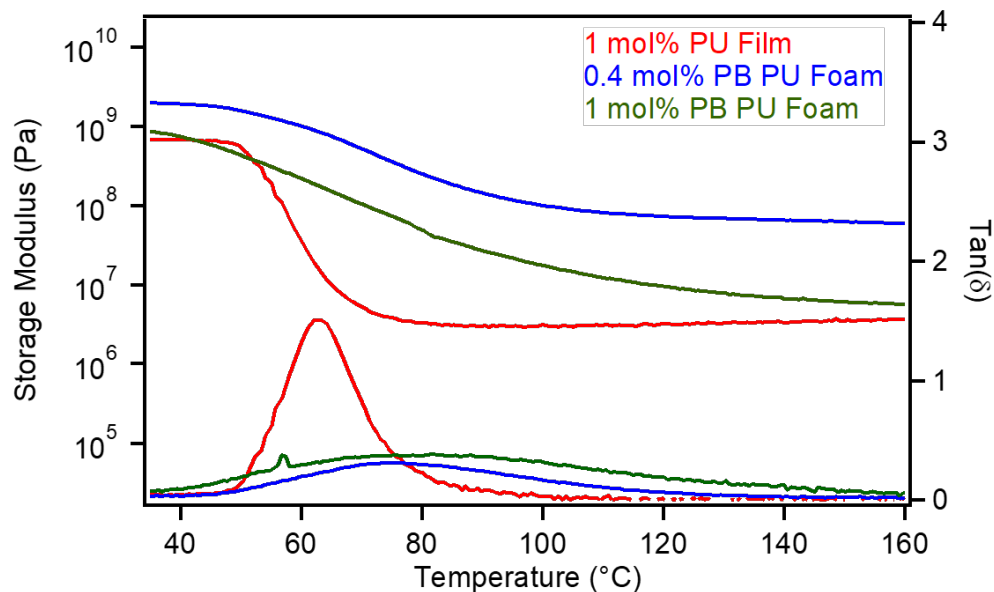


**Figure S6.** DMTA of compression molded PU film containing 1 mol% DBTDL per carbamate (red), compression molded PB PU foam containing 0.4 mol% DBTDL (blue), and compression molded PB PU foams containing 1 mol% DBTDL (green). Foams and films were directly synthesized with the catalyst and were not post-synthetically treated with DBTDL solution.

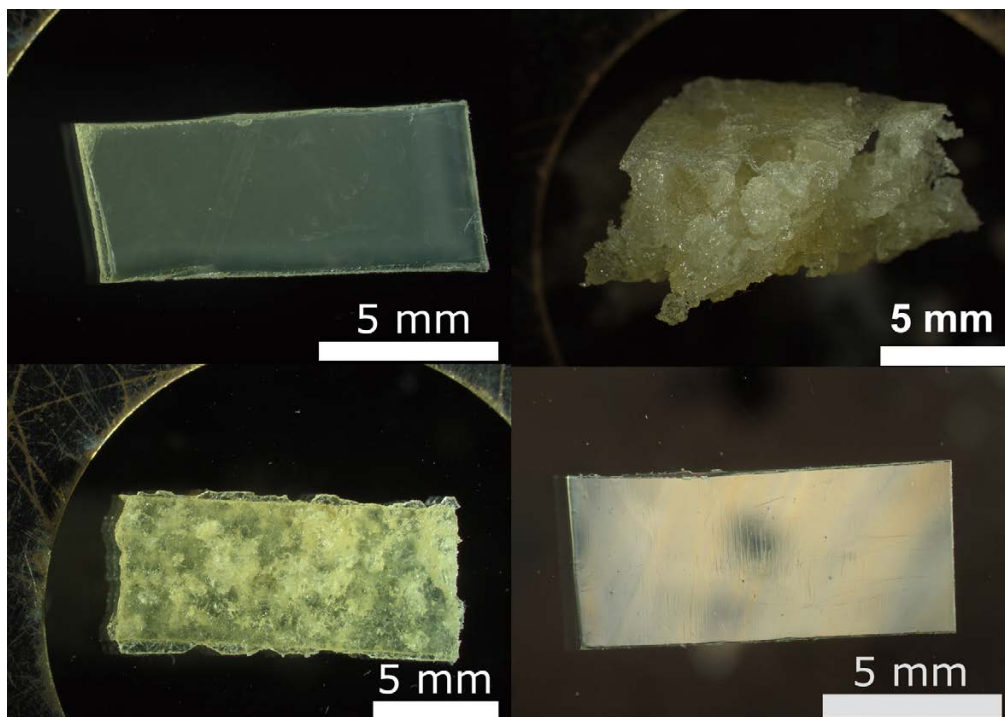


**Figure S7.** Optical microscopic images of as-synthesized PU film (top left), PB PU foam (top right), model PB foam compression molded (bottom left), and PB PU foam microcompounded (bottom right).

**Table S2.** Tensile testing of DBTDL polyester polyurethanes before and after reprocessing

Model Foams	$\sigma_b$ (MPa)	$\gamma_p$ (%)	$E$ (GPa)
As-Synthesized	$49.7 \pm 1.6$	$4.8 \pm 1.0$	$1.57 \pm 0.09$
Compression Molded	$13.6 \pm 1.4$	$1.4 \pm 0.1$	$1.04 \pm 0.11$
Start of Extrudate	$50.8 \pm 6.7$	$3.6 \pm 1.0$	$1.89 \pm 0.18$
End of Extrudate	$47.1 \pm 12.1$	$3.2 \pm 1.1$	$2.20 \pm 0.30$

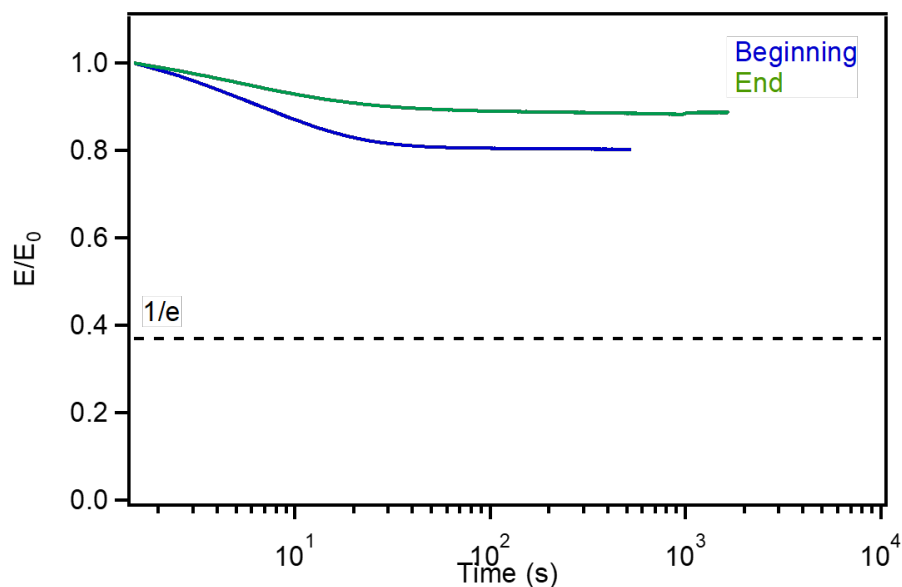


**Figure S8.** Representative SRA traces at 160 °C of microcompounded physically blown foam post-synthetically treated with DBTDL at the start (blue) and end (green) of the extrudate.

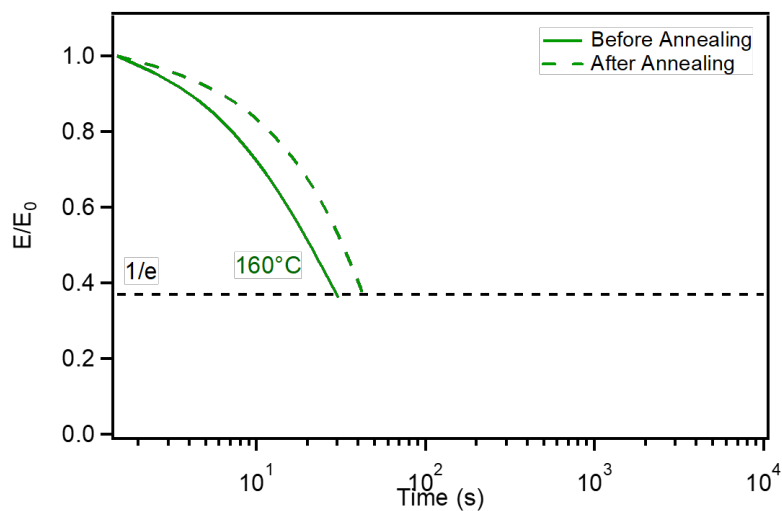


**Figure S9.** Representative SRA of PU film containing DBTDL before annealing (solid line) and after annealing (dashed line) at 200 °C for 2 minutes under air. Temperature was chosen to mimic microcompounding temperature.



**Figure S10.** Representative images of microcompounded PB PU foam using  $\text{Bi}(\text{neo})_3$ . The light portions are the earliest portion of the extrudate whereas the darker portions of the extrudate are the latest portion. Extrusion is non-continuous and stops when the microcompounder reaches its torque limit.

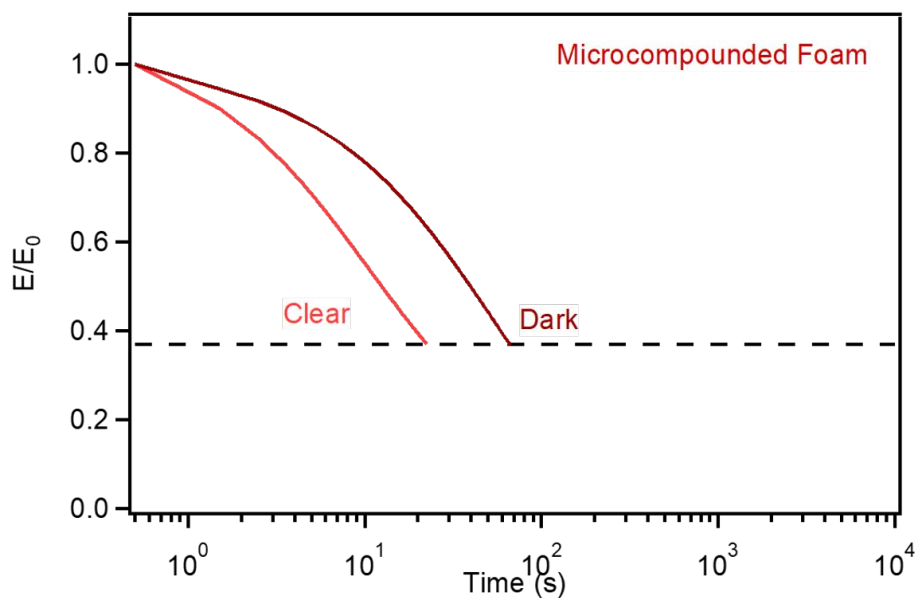


**Figure S11.** Representative SRA of microcompounded PB PU foam containing  $\text{Bi}(\text{neo})_3$  at 200 °C until the torque limit is reached. The clear portion of the extrudate is the earliest part of the extrudate whereas the dark portion of the extrudate is the late portion.

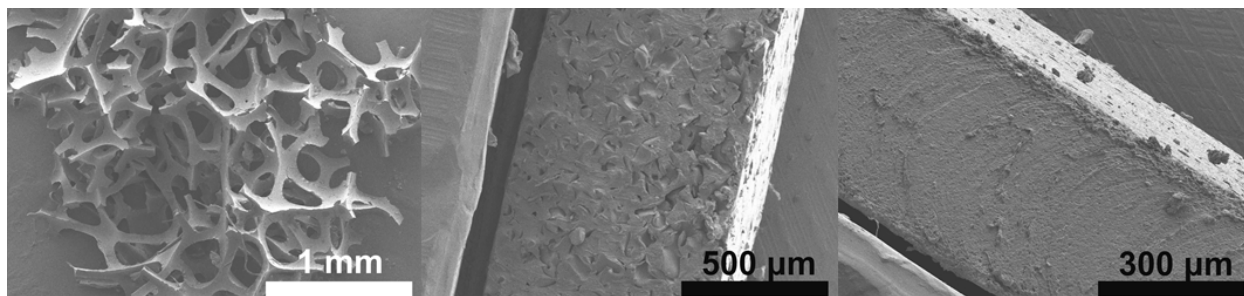


**Figure S12.** SEM images of commercial PU flexible foam (left), compression molded commercial PU foam (middle), and microcompounded commercial PU foam (right)



**Figure S13.** Attempted microcompounding of commercial PU foam without introducing catalyst using solution swelling.



**Figure S14.** Optical microscopic images of commercial PU flexible foam (left), compression molded commercial PU foam (middle), and microcompounded commercial PU foam (right)

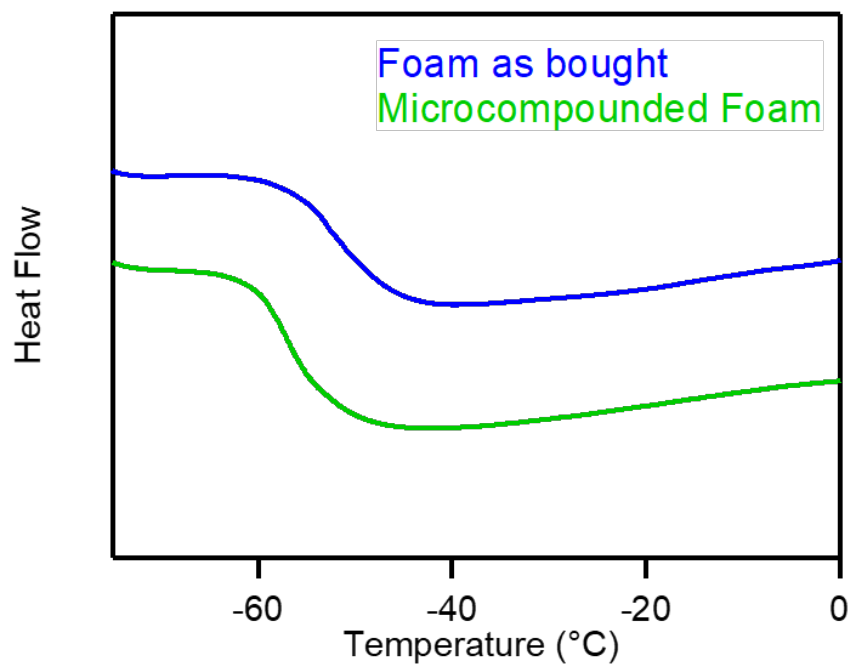


**Figure S15.** Differential scanning calorimetry of commercial foam as bought (blue) and after microcompounding (green).

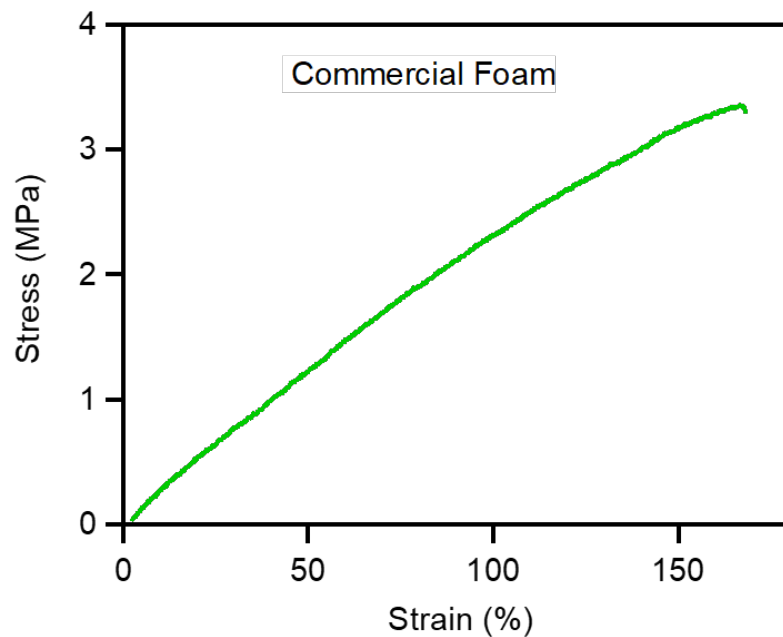


**Figure S16.** Tensile testing of microcompounded commercial (AirLite) foam.

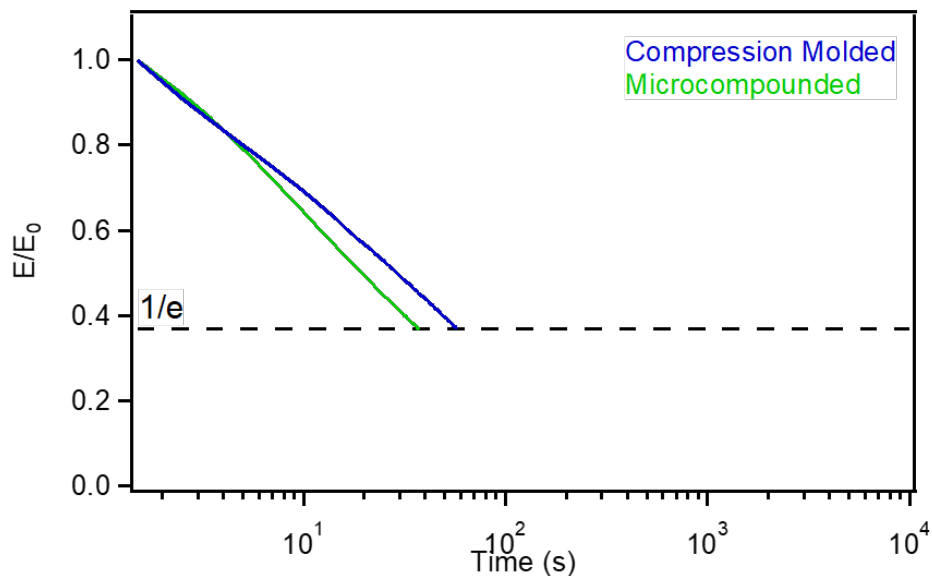


**Figure S17.** SRA of compression molded (blue) and microcompounded (green) commercial (AirLite) foam at 160 °C.

**Table S3.** Characterization table of model PU materials

Model PU materials	Gel Frac	$T_d$ (°C, 5%)	$T_{g,DSC}$ (°C)	$T_{g,DMTA}$ (°C)	$E'$ at 110 °C (MPa)	Tan( $\delta$ ) area	Peak of tan( $\delta$ )	Density (g/cm <sup>3</sup> )	$E_a$ (kJ/mol)
As-Synthesized PU Films	87	284	45	53	3.08	28.3	1.56 63 °C	1.13 ± 0.03	143 ± 5
As-Synthesized PB Foam	89	260	61	-	-	-	-	0.31 ± 0.02	-
Compression Molded PB Foam	-	-	-	60	80.8	17.2	0.32 75 °C	1.02 ± 0.04	159 ± 6
Microcompounded PB Foam	99	210	57	52	3.18	36.0	1.27 69 °C	1.33 ± 0.08	-

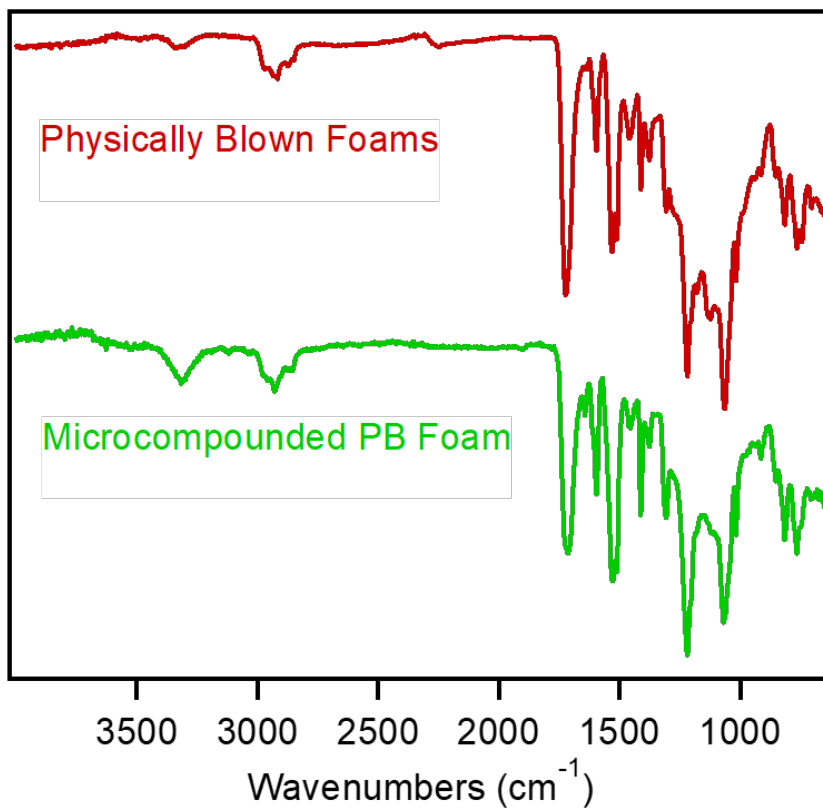


**Figure S18.** FT-IR of synthesized physically blown foams (red) and subsequently microcompounded physically blown foams (green).

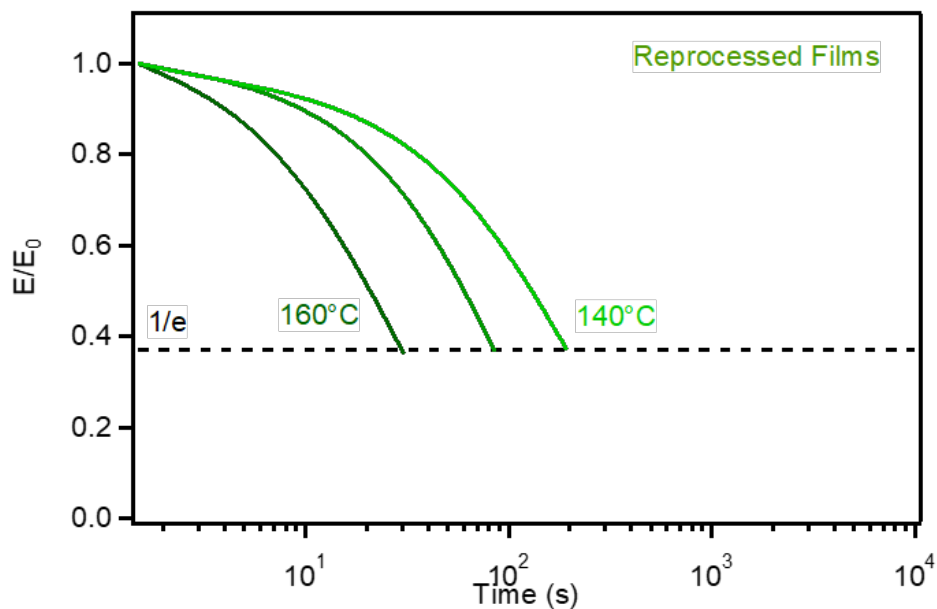


**Figure S19.** Representative SRA traces (140, 150, and 160 °C) of model PU films post-synthetically treated with DBTDL, then compression molded for 12 min at 160 °C.

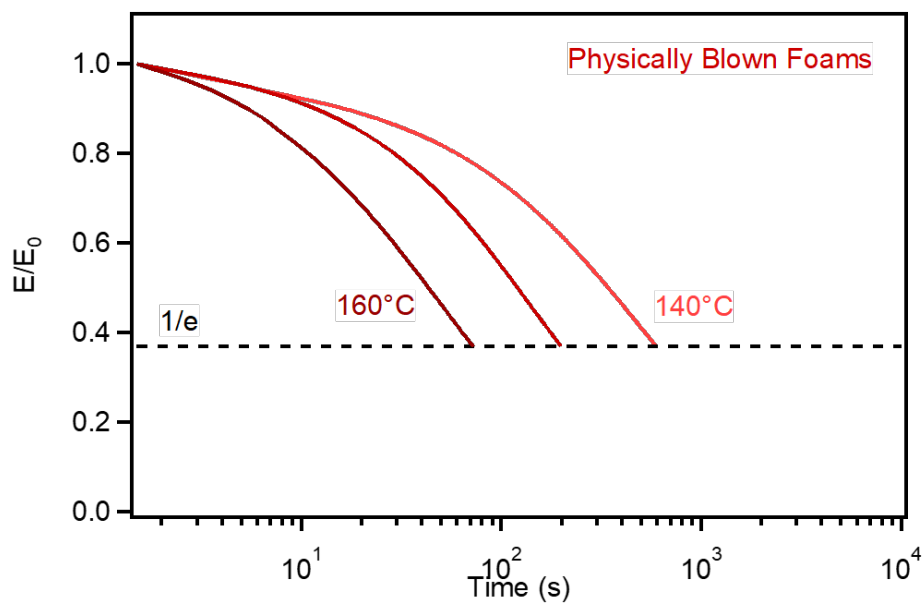


**Figure S20.** Representative SRA traces (140, 150, and 160 °C) of model physically blown PU foams post-synthetically treated with DBTDL, then compression molded for 12 min at 160 °C.

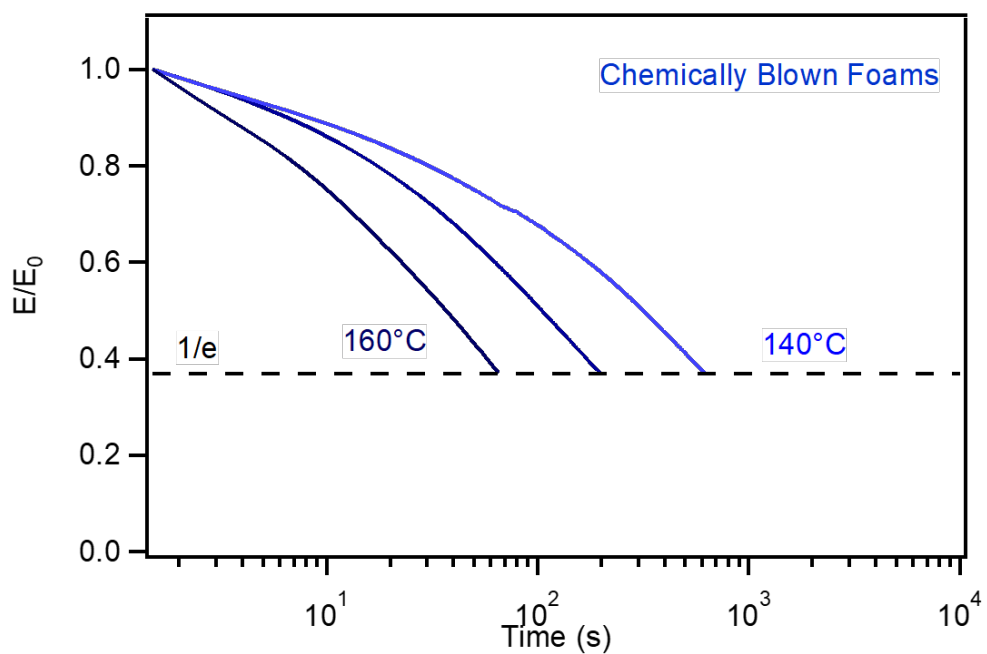


**Figure S21.** Representative SRA traces (140, 150, and 160 °C) of model chemically blown PU foams post-synthetically treated with DBTDL, then compression molded for 12 min at 160 °C.



**Table S4.** Characteristic relaxation times of compression molded model PU materials at various temperatures.

Material Type	160 °C	150 °C	140 °C
<b>Films</b>	28 ± 1 s	82 ± 3 s	194 ± 9 s
<b>PB Foam</b>	71 ± 4 s	226 ± 20 s	605 ± 11 s
<b>CB Foam</b>	53 ± 16 s	206 ± 25 s	642 ± 113 s

**Table S5.** Characterization table of commercial PU foam

Commercial Foam	Gel %	$T_d$ (°C, 5%)	Area of $\tan(\delta)$ curve	Peak of $\tan(\delta)$	$T_{g,DSC}$ (°C)	$T_{g,DMTA}$ (°C)	$E'$ at 40 °C (MPa)
As Supplied	98	254	-	-	-49	-	-
Compression molded	-	-	22.1	0.40 -43 °C	-	-48	18.9
Microcompounded	85	255	32.7	0.63 -45 °C	-55	-55	3.43

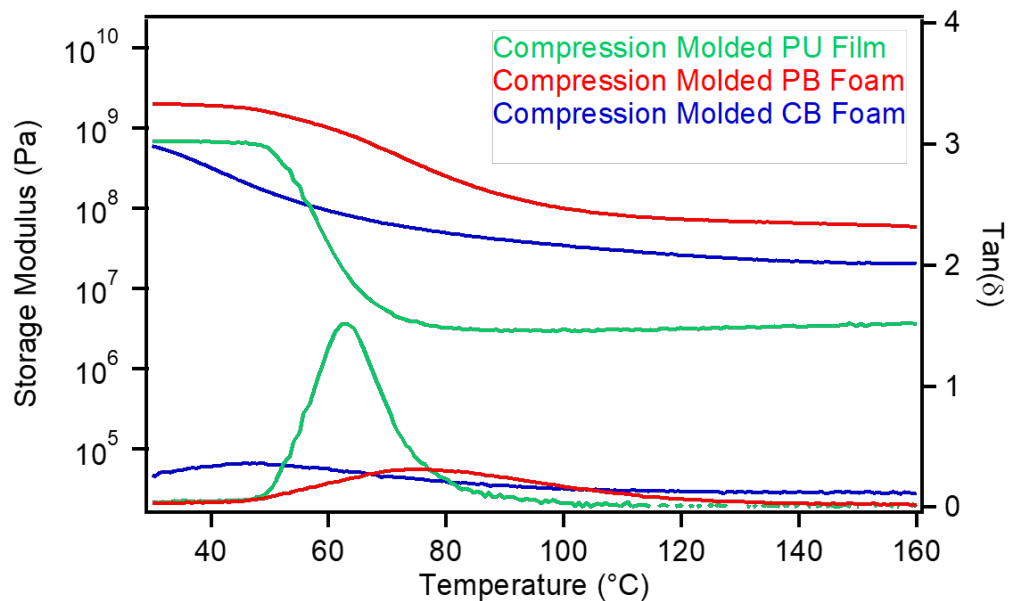


**Figure S22.** Dynamic mechanical thermal analysis of compression molded PU film (green), PB foam (red), and CB foam (blue)

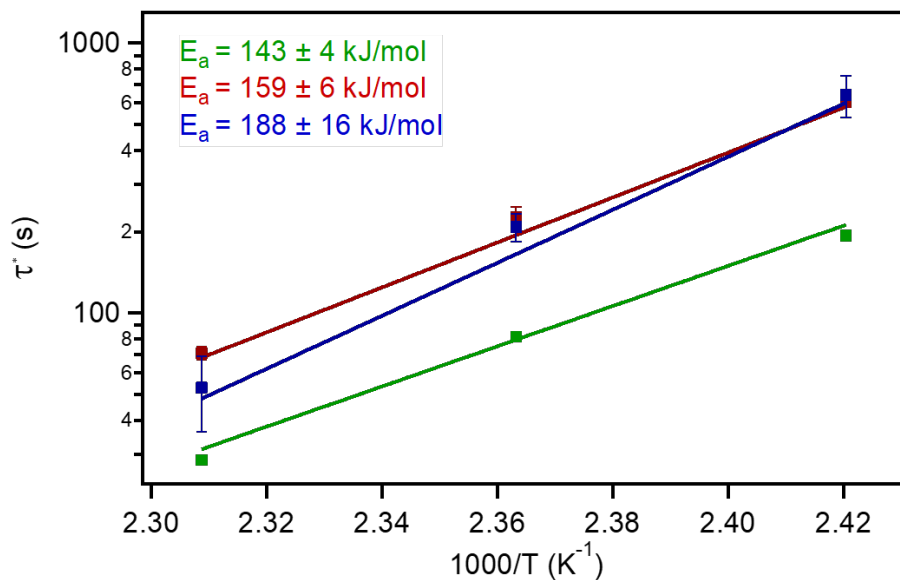


**Figure S23.** Activation energies of stress relaxation in compression molded PU film (green), PB foam (red), and CB foam (blue).

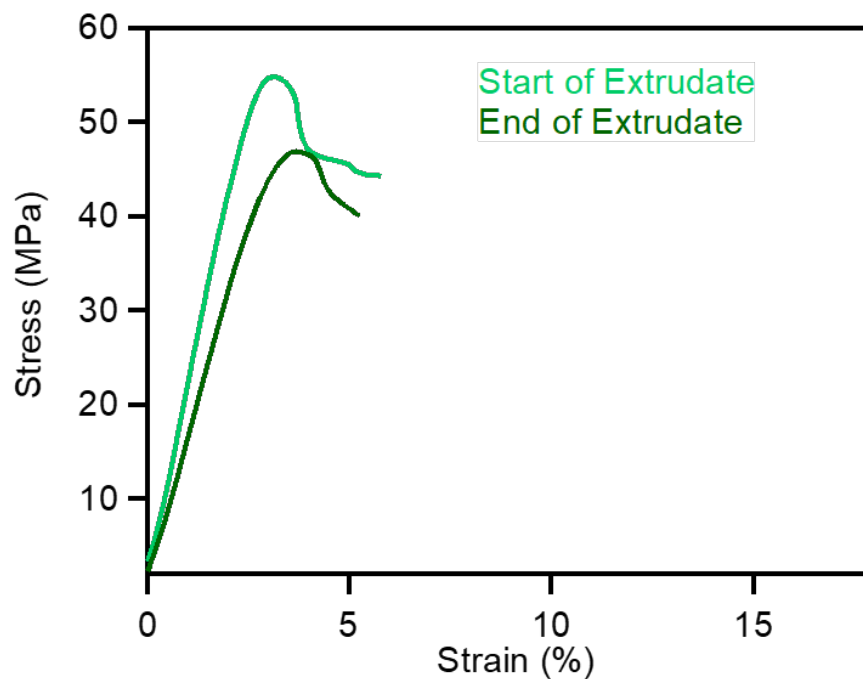


**Figure S24.** Tensile testing of microcompounded PB PU foam at the start of the extrudate (light green) to the end of the extrudate (dark green).

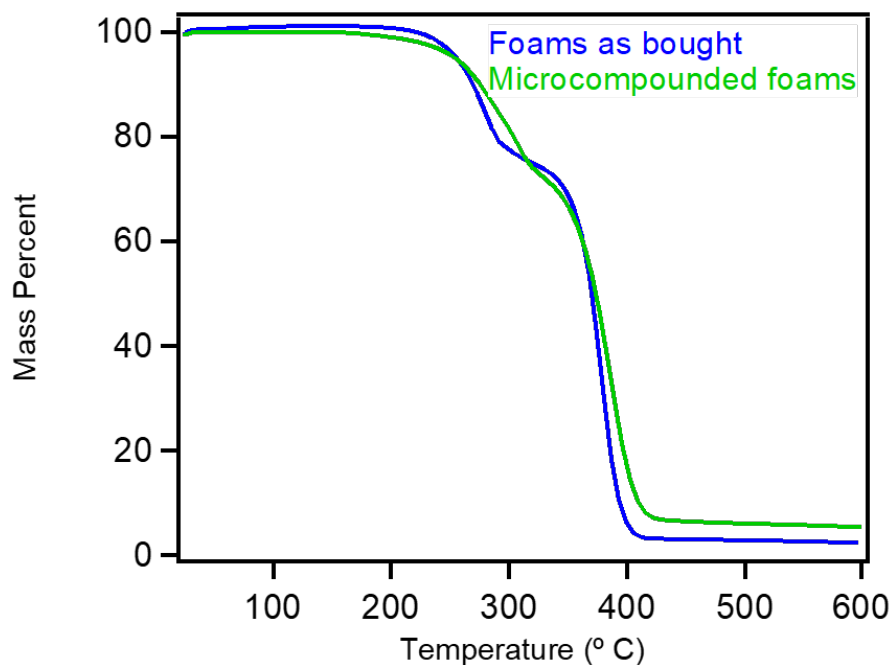


**Figure S25.** Thermogravimetric analysis of as-synthesized films (blue), physically blown PU foams (red), and commercial PU foams (green).

**Table S6.** Tensile testing averages of microcompounded commercial (AirLite) foam

Commercial Foams	$\sigma_b$ (MPa)	$\epsilon_b$ (%)	$E$ (MPa)
Microcompounded	$3.3 \pm 0.3$	$155 \pm 9$	$2.86 \pm 0.30$

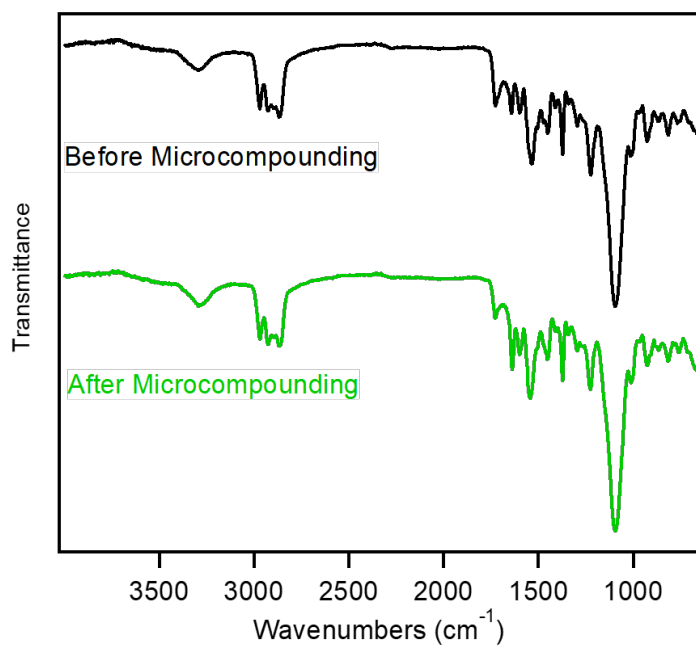


**Figure S26.** FT-IR of commercial PU foam before and after microcompounding.

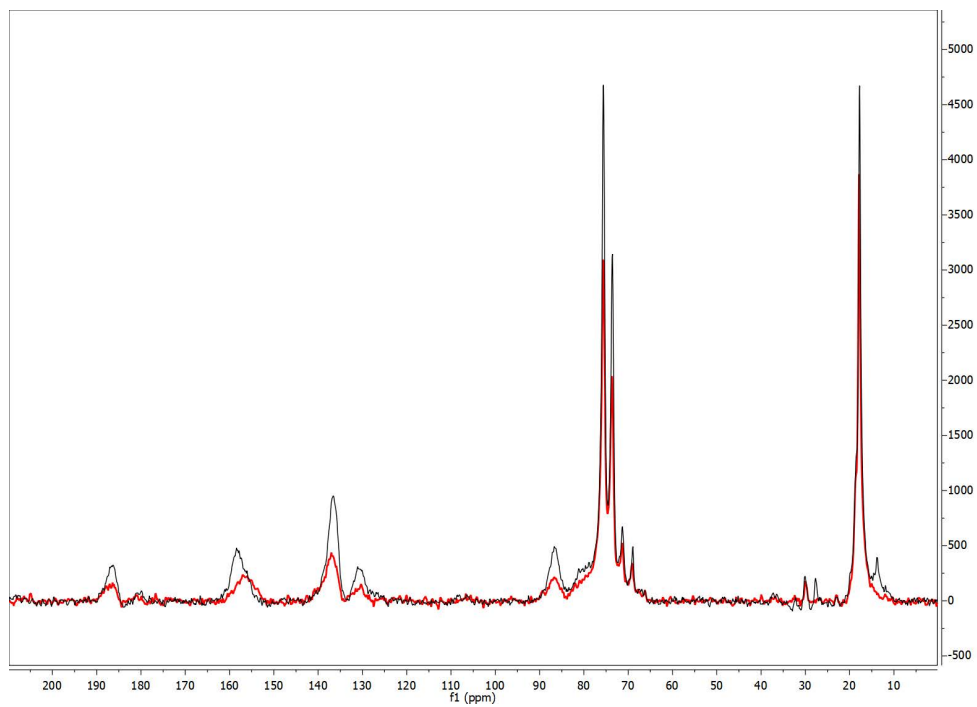


**Figure S27.** Solid state  $C^{13}$  NMR of commercial PU foam before (red) and after microcompounding (black).



**Figure S28.** Attempted compression molding of catalyst-containing commercial PU foam showing poor processability.

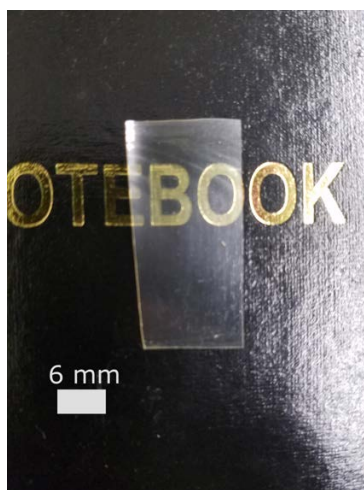


**Figure S29.** Image of microcompounded PB PU foam into film.



**Figure S30.** Representative image of synthesized model PU foam.

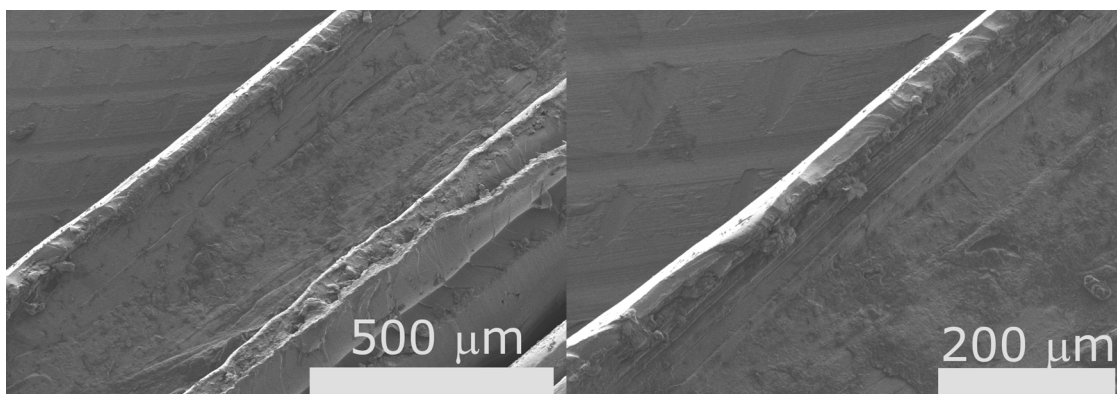


**Figure S31.** SEM images of compression molded model PU film at lower magnification (left) and higher magnification (right) for 12 minutes showing the absence of voids.

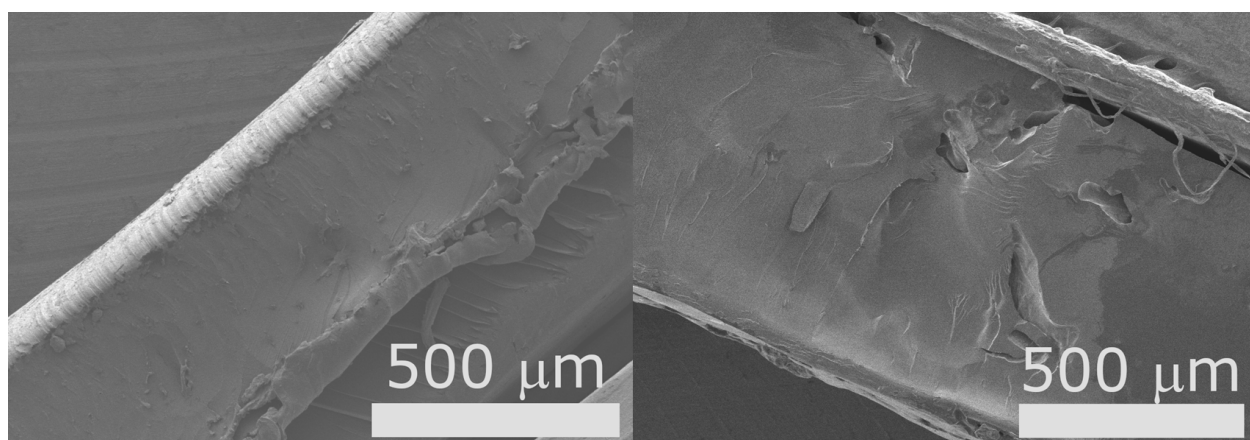


**Figure S32.** SEM of compression molded PU model films and compression molded PB PU foams for 1 hour.



**Figure S33.** Attempted reprocessing of as-synthesized PU film without any catalyst present.

## D. References

1. Brutman, J. P.; Delgado, P. A.; Hillmyer, M. A., Polylactide Vitrimers. *ACS Macro Letters* **2014**, 3 (7), 607-610.
2. Menard, K. P.; Menard, N. R., Dynamic Mechanical Analysis in the Analysis of Polymers and Rubbers. In *Encyclopedia of Polymer Science and Technology*, 2015; pp 1-33.